

ASSEMBLY DIMENSIONAL VARIATION MODELING AND OPTIMIZATION FOR RESIN TRANSFER MOLDING PROCESS

Chensong Dong, Chuck Zhang, Zhiyong Liang and Ben Wang
Department of Industrial Engineering
Florida A&M University-Florida State University College of Engineering
Tallahassee, FL 32310-6046

ABSTRACT

The increasing demand for composite products to be affordable, net-shaped and efficiently assembled makes tight dimensional tolerance is critical. Due to lack of accurate process models, RTM dimensional analysis and control are often performed using trial-and-error approaches based on engineers' experiences or previous production data. Such approaches are limited to specific geometry and materials and often fail to achieve the required dimensional accuracy in the final products. This paper presents an innovative study on the dimensional variation prediction and control for polymer matrix fiber reinforced composites. A dimensional variation model was developed for process simulation based on thermal stress analysis and finite element analysis (FEA). This model was validated against the experimental data, the analytical solutions and the data from literature. Using the FEA-based dimensional variation model, the deformations of typical composite structures were studied and the regression-based dimensional variation model was developed. By introducing the material modification coefficient, this comprehensive model can account for various fiber/resin types and stacking sequences. The regression-based dimensional variation model can significantly reduce computation time by eliminating the complicated, time-consuming finite element meshing and material parameter defining process, which provides a quick design guide for composite products with reduced dimensional variations. The structural tree method (STM) was developed to compute the assembly deformation from the deformations of individual components, as well as the deformation of general shape composite components. The STM enables rapid dimensional variation analysis/synthesis for complex composite assemblies with the regression-based dimensional variation model. The exploring work presented in this research provides a foundation to develop practical and proactive dimensional control techniques for composite products.

KEY WORDS: Dimensional variation, Resin Transfer Molding (RTM), Finite Element Analysis (FEA), regression, Structural Tree Method (STM)

1 INTRODUCTION

The applications of composites are important in both commercial and military products due to their structural and functional features. With the increasing demand for composite products to be affordable, net-shaped and efficiently assembled, tight dimensional tolerances are often required. Traditional dimensional control operations for composites are mainly based on trial-and-error approaches, which cannot be directly and effectively employed in real world part design and tooling development. In another aspect, the increasing applications of new processes, such as resin transfer molding (RTM) and vacuum assisted resin transfer molding (VARTM), will also

raise a number of new issues in dimensional control. For example, large warpage in RTM process is observed due to the occurrences of resin rich surfaces and resin rich zones.

The problem of dimensional variations for composite parts comes from the volumetric shrinkage of the resin during curing and the mismatch in the coefficients of thermal expansion of the matrix and the fiber. Primary causes include crosslinking, non-uniform thermal expansion, shrinkage and residual stresses induced in the curing and cooling processes.

The dimensional variations of composites have been studied experimentally [1-3], analytically [4-11] and numerically [12-20].

For simple geometric structures as “L-shaped,” the two curved sides approach each other and this leads to a reduction in the enclosed angle. This decrease in the enclosed angle is referred as spring-in. This is due to the difference between the in-plane CTE and through-thickness CTE as well as chemical strains. The spring-in has been analytically computed for autoclave process [4-8], RTM process [4-7] and filament winding process [9-11].

In order to predict the spring-in of more complex structures, numerical simulation tools of finite element method or finite difference method have been employed. Theriault *et al* [12] developed a one-dimensional finite difference model to simulate the progression of material properties during the processing of metal-clad, multi-layered, fiber mat reinforced, thermoset resins. The general Classical Lamination Theory was implemented to evaluate the dimensional movement of the composite laminate. The spring-in was predicted using FEM by Wiersma *et al* [13]. His approach includes curing simulation, elastic model and viscoelastic model. Darrow and Smith [14-15] employed finite element method to model the processing induced spring-in in laminated composites. Their model accounted for the mold stretching, thickness shrinkage, and fiber volume fraction gradients. This linear elastic model was able to account for 80% of the observed spring-in for parts ranging between 1 and 5 mm thick and having a 3 to 13 mm bend radius. Golestanian and El-Gizawy [16] modeled the process-induced residual stresses and deformation in composite parts using finite element method coupled with cure-dependent mechanical properties. Wang *et al* [17] conducted finite element method (FEM) analysis to spring-in using ABAQUS. Fernlund *et al.* [18] presented an engineering approach to predict process-induced deformations of three-dimensional composite shell structures, using a two-dimensional special purpose finite element process code COMPRO and a standard three-dimensional structural code ANSYS.

A number of full 3-D spring-in models have been developed recently. Ding *et al.* [19] developed a 3-D finite element analysis procedure to predict “spring-in” resulting from anisotropy for both thin and thick angled composite shell structures. Zhu *et al.* [20] developed a fully 3-D coupled thermo-chemo-viscoelastic finite element model to simulate the heat transfer, curing, and residual stress development during the manufacturing cycle of thermoset composite parts.

From the literature review, it is seen that many studies have focused on the curing process and residual stresses in composite processing. Various models were proposed for the deformation prediction of composite structures. However, most of them were based on finite element analysis and they are not convenient for industry applications. The influence of design on the

dimensional variations has not been fully investigated, which is necessary to achieve good dimensional control in the early design stage. In addition, the prediction and control for deformations of composite assemblies lack a thorough study. Thus, it is highly desirable to develop an engineering tool for composite component and assembly design with good dimensional control.

In this study, a regression-based dimensional variation model was developed based on the study of typical composite structures using the FEA-based dimensional variation model. The structural tree method (STM) was developed to compute the deformations of general shape composite components and composite assemblies. By using the regression-based dimensional variation model and the structural tree method, the dimensional variations of composite products and assemblies can be predicted effectively and efficiently.

2 FEA-BASED DIMENSIONAL VARIATION MODEL

For the purpose of deformation prediction for part produced with the RTM process, a dimensional variation model [21-23] was developed and validated. The approach is illustrated in Figure 1. A non-isothermal flow and curing model was developed to simulate the flow pattern and temperature distribution. A material model was used to compute the material properties, i.e. CTE, moduli, etc. These results, with the design geometry and processing parameters, were imported into the dimensional variation model, which was based on the CLT and FEA, to compute the deformation. Using the same design geometry, material properties and processing parameters, experimental parts were fabricated and measured using a coordinate measuring machine (CMM) for the purpose of validation. The measured data and the computational results were compared, where in Figure 1, d_{com} is the computational results and d_{exp} is the experimental result. The model parameters were revised to provide a prediction as accurate as possible.

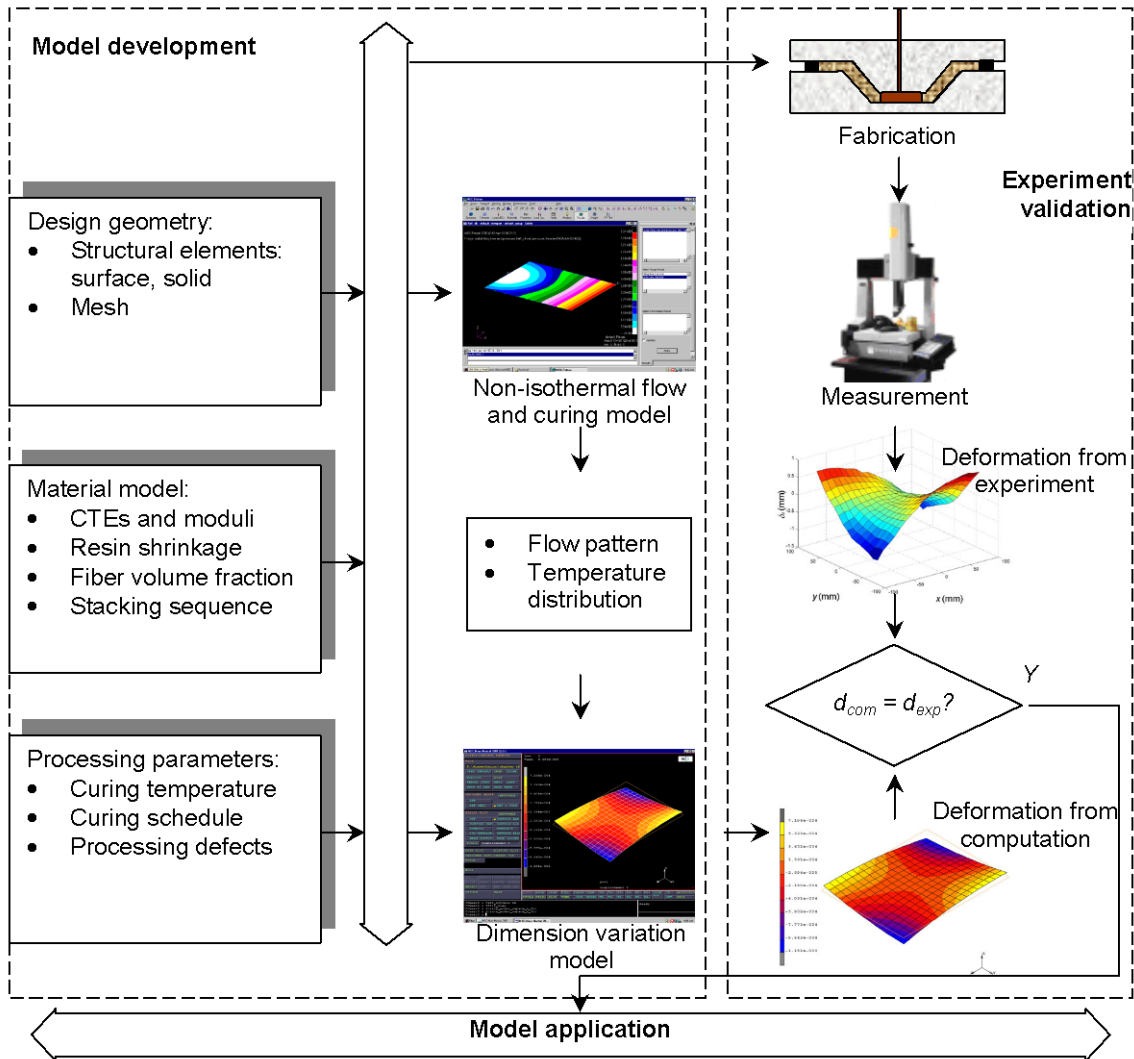


Figure 1: Model development and validation

In order to validate the developed FEA-based dimensional variation model, a single-stiffener, as shown in Figure 2, was studied. The mold assembly is shown in Figure 3. Experimental parts were fabricated from E-glass fiber mats and epoxy resin. First, a $[0/90]_s$ laminate was studied. The fiber volume fraction was determined experimentally. Before the experiment, the fiber mats were weighed using a scale. The mass was 36.8g; after the part was fabricated, as shown in Figure 4, the final part was weighed and the mass was 101.11g. The fiber volume fraction was 22%. This data was used in the material model.

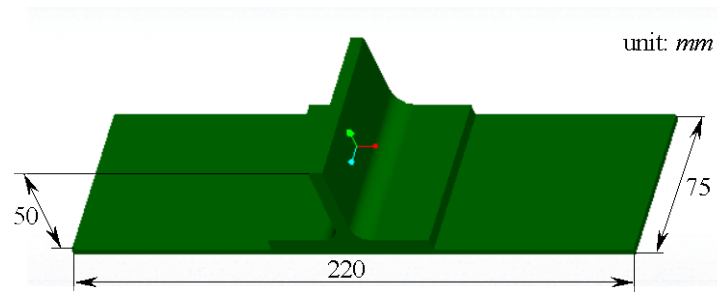


Figure 2: A single-stiffener structure

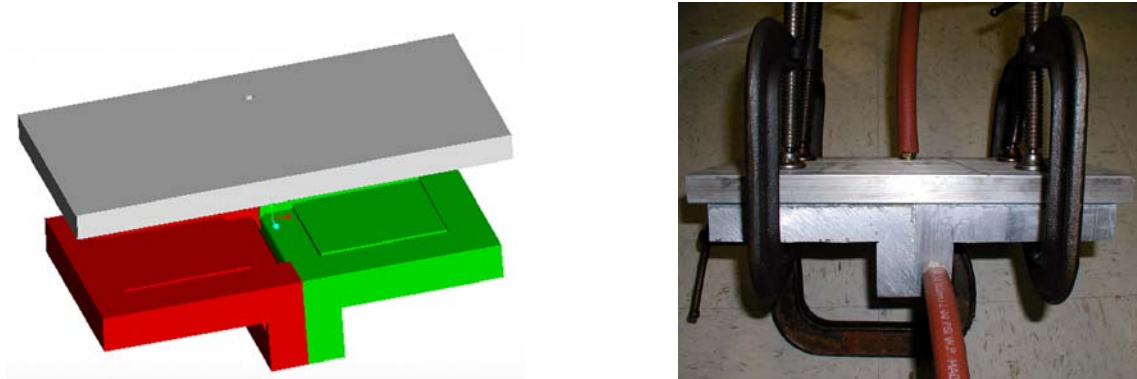


Figure 3: Mold assembly for the single-stiffener structure

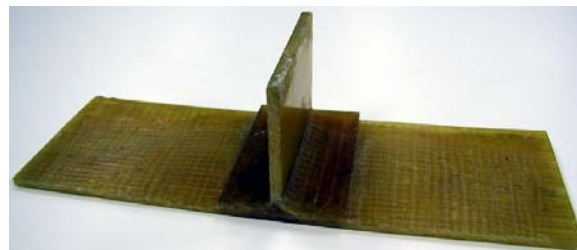


Figure 4: A finished single-stiffener part

After the thickness was determined, the single stiffener structure was modeled. Due to the lay-up of fiber mats, resin rich zones were formed, as shown in Figure 5, which were accounted for in modeling. Half of the structure was modeled and the symmetric boundary condition was applied. The FEA result is shown in Figure 6, where the contours indicate the total displacement in mm. The spring-in angle is -0.49° .

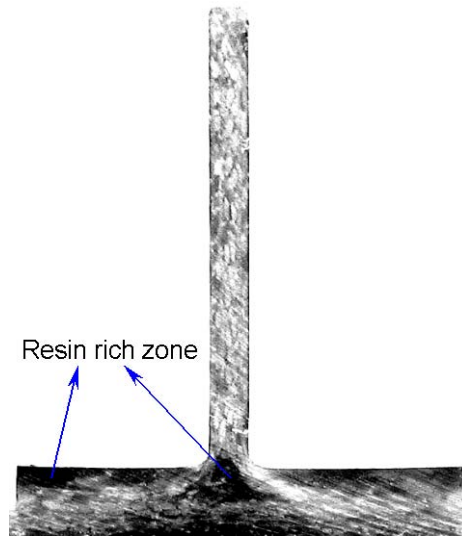


Figure 5: Resin rich zones

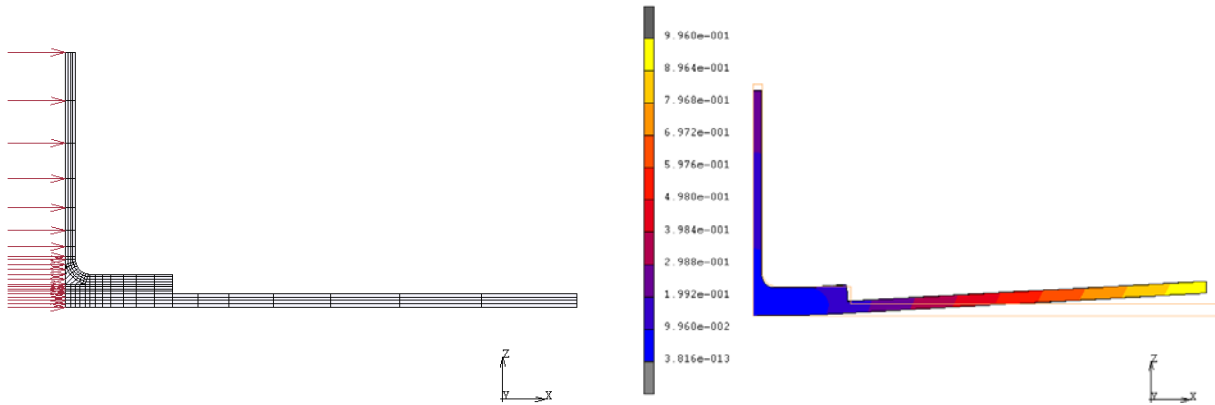


Figure 6: FEA result for the single-stiffener structure
Left: mesh; right: dimensional variation

The spring-in angle was measured 10 times on the CMM, as shown in Figure 7. The measurement data is shown in Table 1. The average of the spring-in angle is -0.52° .

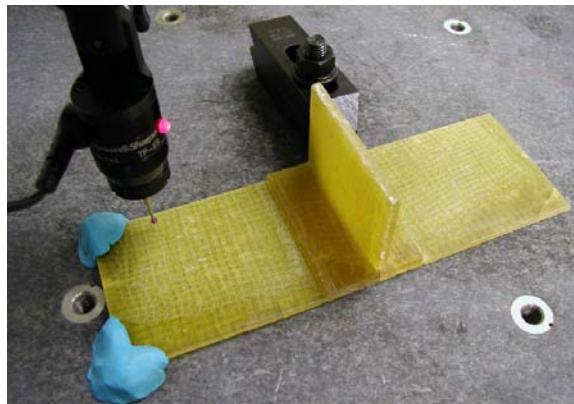


Figure 7: Spring-in measurement of the single-stiffener part

Table 1: Spring-in measurement of single-stiffener

| n | spring-in ($^{\circ}$) |
|---------|--------------------------|
| 1 | -0.506 |
| 2 | -0.466 |
| 3 | -0.616 |
| 4 | -0.595 |
| 5 | -0.469 |
| 6 | -0.436 |
| 7 | -0.493 |
| 8 | -0.481 |
| 9 | -0.516 |
| 10 | -0.632 |
| average | -0.521 |

In the same approach, a unidirectional laminate of $[90]_4$ was studied. The results were compared with the computational results as shown in Table 2. Both cases show that the experimental data agree with the computational results.

Table 2: Comparison between computational results and experimental results for the single-stiffener E-glass/epoxy parts

| | Computational result ($^{\circ}$) | Experimental result ($^{\circ}$) | Relative error |
|------------|-------------------------------------|------------------------------------|----------------|
| $[0/90]_s$ | -0.49 | -0.52 | 6% |
| $[90]_4$ | -0.063 | -0.080 | 20% |

The model validation shows that despite the existence of certain amount of errors, the model is capable of accurately predicting the deformation trends of composites.

3 TYPICAL COMPOSITE STRUCTURE STUDY AND REGRESSION-BASED DIMENSIONAL VARIATION MODEL

The deformation of composites can be computed using the developed dimensional variation model. However, this approach is FEA-based. The FEA for composite modeling involves a complicated geometric modeling and meshing process, as well as a large amount of parameter input work due to the layer-wise structure of composites. This requires extensive FEA knowledge and skills for users. The computation is often time-consuming when the geometry becomes complex and the number of nodes and elements becomes large. All of these limit its applications in industry. Thus, typical composite structures were investigated and the influences of design parameters on the deformation were studied. The regression-based dimensional variation model was developed.

The deformation of composites is related to design geometric parameters, material parameters and processing parameters. This gives us a functional relationship as

$$\delta = f(G, M, P) \quad (1)$$

where





δ : deformation vector
 G : design geometric parameters
 M : material parameters (fiber, resin)
 P : processing parameters (temperature, curing)

Since geometry is one of the primary factors determining the deformation of composites, research attention can be focused onto several typical structures such as angled structures, stiffener structures, etc. The purpose is to relate their deformations with the structural parameters and develop a regression-based dimensional variation model.

3.1 Selection of Typical Structures

First, the materials were fixed (E-glass/epoxy) in order to study the effects of geometric parameters. Based on experience, seven commonly used typical structures were chosen, as shown in Table 3, together with their corresponding tolerances and design parameters. The developed dimensional variation model was used to simulate the deformation of composites. Data were collected by modifying the geometric parameters such as radius and thickness. Non-linear regression models were developed based on these collected data.

Table 3: Typical structures and design parameters

| Typical structure | Tolerances | Design parameters |
|---|---------------------------------|---|
|  Angled structure | Perpendicularity Angularity | Angle ϕ Radius r Thickness h |
|  Single-stiffener structure | Perpendicularity | Radius r Thickness h |
|  Multiple-stiffener structure | Perpendicularity Parallelism | Radius r Thickness h |
|  Cylindrical shell | Cylindricity | Radius r Thickness h |

3.2 An Example: a Single-Stiffener Structure

A single-stiffener structure was used to illustrate the approach. The spring-in of the single-stiffener structure is controlled by the perpendicularity. With reference to Figure 8, the design parameters possibly affecting the perpendicularity are the half-length $L/2$, the height H ,

the inner radius r , and the thickness h . The perpendicularity is proportional to the half-length of the structure, $L/2$. Thus, the spring-in angle was investigated alternatively to reduce the number of design parameters. It is related to the perpendicularity as

$$T_{pe} = L\Delta\phi/2 \quad (2)$$

where T_{pe} is the perpendicularity; $L/2$ is the half-length of the single-stiffener structure; and $\Delta\phi$ is the spring-in angle.

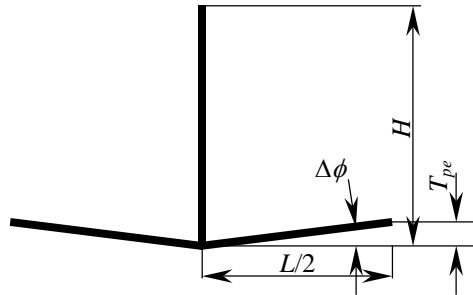


Figure 8: Tolerances of the single-stiffener structure

The cross ply E-glass/epoxy laminates were first studied. First, the fiber volume fraction was fixed at 49%. The design parameters and levels are shown in Table 4.

Table 4: Design parameters and levels for single-stiffener structures

| Thickness h (mm) | Radius r (mm) | Fiber volume fraction V_f |
|--------------------|-----------------|-----------------------------|
| 1.058 | 3.175 | 0.41 |
| 2.117 | 6.35 | 0.49 |
| 3.175 | 9.525 | 0.57 |
| 4.233 | — | 0.66 |

The spring-in was simulated using the FEA-based dimensional variation model. When the thickness is 2.117 mm and the inner radius is 6.35 mm, the FEA result is shown in Figure 9. The spring-in is -0.14° . The complete results for all cases are shown in Figure 10. The spring-in angle increases linearly with the increase of inner radius r and decreases exponentially with the increase of thickness h . This is because of the existence of resin rich zones. The resin shrinks much more than the lamina, and its modulus is much lower than that of the lamina.

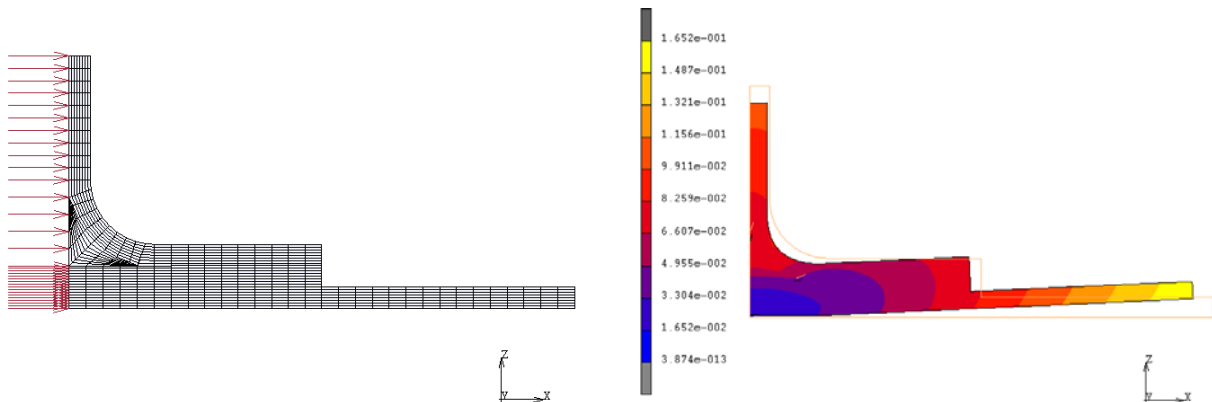


Figure 9: FEA result for the single-stiffener structure
Left: mesh; right: dimensional variation

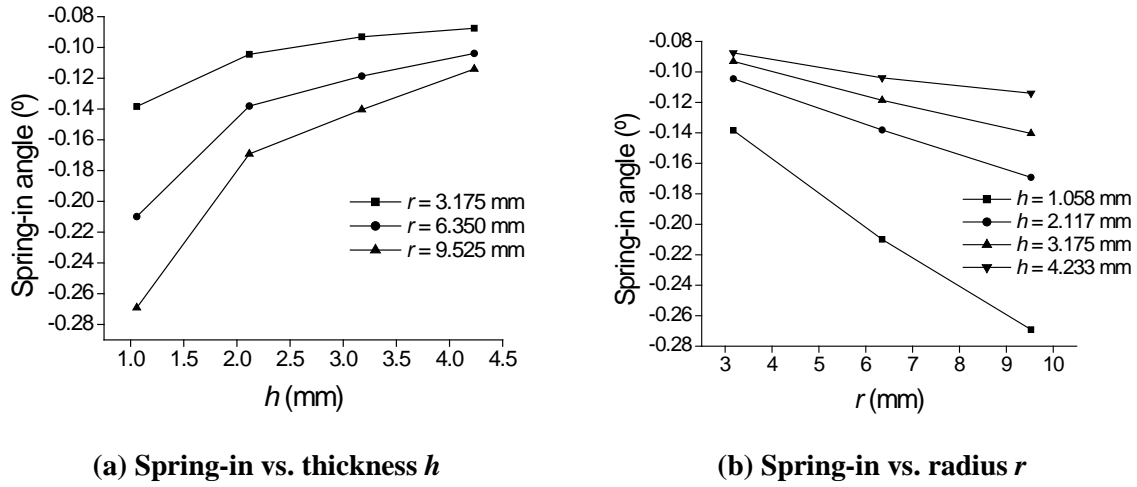


Figure 10: Influences of radius and thickness on the spring-in of single-stiffener structures

In addition, the effect of fiber volume fraction was also studied. The results are shown in Figure 11. The spring-in angle decreases with the increase of the fiber volume fraction.

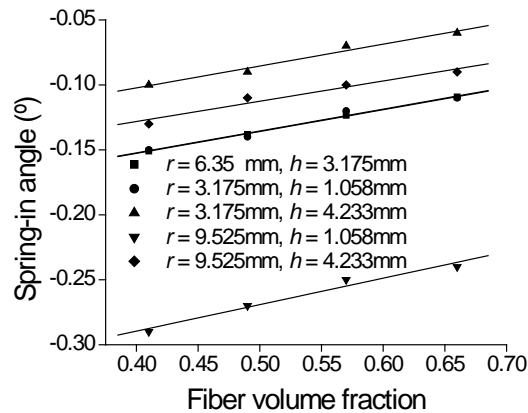


Figure 11: Influence of fiber volume fraction on the spring-in of single-stiffener structures

Similarly, in order to reveal the effects of the stacking sequence, the spring-in of symmetric angle ply laminates was investigated. In the study cases, the inner radius is 3.175 mm, 6.35 mm, and 9.525 mm, respectively; and the thickness is 2.117 mm. The results are shown in Figure 12. When the fiber orientation changes from 0 to 90°, the difference between the in-plane CTE and the through-thickness CTE decreases, thus the spring-in angle decreases.

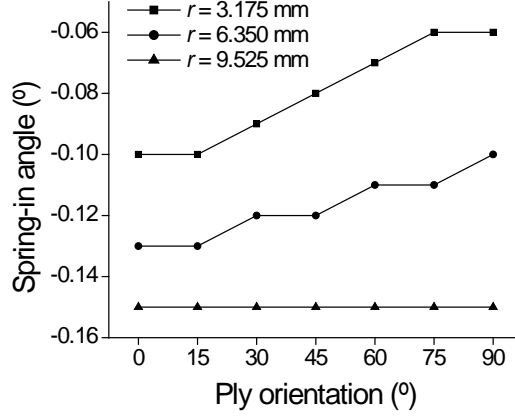


Figure 12: Spring-in of angle ply E-glass/epoxy laminates $[\theta-\theta]_{ns}$

By examining the curves of $\Delta\phi$ vs. r , linear relationships exhibit. Thus, linear regression models were developed as follows for $h = 1.058$ mm to 4.233 mm, respectively.

$$\Delta\phi = -0.075 - 0.021r, \quad (h = 1.058 \text{ mm}) \quad (3a)$$

$$\Delta\phi = -0.073 - 0.010r, \quad (h = 2.117 \text{ mm}) \quad (3b)$$

$$\Delta\phi = -0.070 - 0.007r, \quad (h = 3.175 \text{ mm}) \quad (3c)$$

$$\Delta\phi = -0.075 - 0.004r. \quad (h = 4.233 \text{ mm}) \quad (3d)$$

Equation 3 shows that the constant term is nearly constant for the four cases. When examining the slope, an exponential decay relationship exhibits. Thus, the slopes can be regressed using an exponential decay model. The regression model for $V_f = 49\%$ is

$$\Delta\phi = -0.073 - \left(0.003 + 0.040e^{-\frac{h}{1.264}} \right) r. \quad (4)$$

By examining the curves of $\Delta\phi$ vs. fiber volume fraction, linear relationships exist and the slopes are nearly the same. Thus the final regression model for the spring-in of E-glass/epoxy single-stiffener structures is

$$\Delta\phi = -0.073 - \left(0.003 + 0.040e^{-\frac{h}{1.264}} \right) r + 0.173(V_f - 0.49). \quad (5)$$

The fitted values and original values are compared in Figure 13. The relative errors are within $\pm 7\%$.

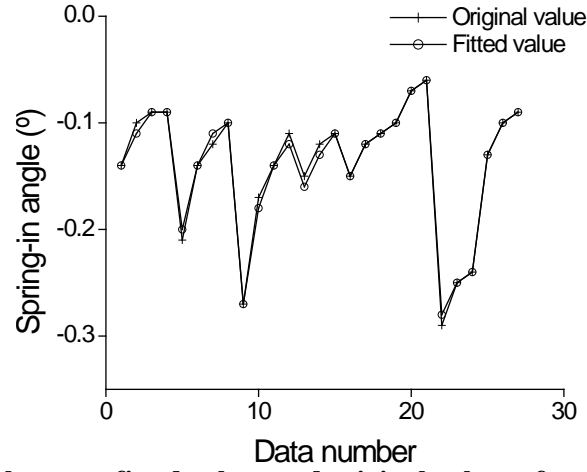


Figure 13: Comparison between fitted values and original values of spring-in for single-stiffener structures

3.3 Regression Models for Other Fiber/Resin Systems

After the regression models for E-glass/epoxy laminates were developed, they were expanded to other fiber/resin systems. When other fiber/resin systems are used, these regression models need to be revised. Based on thermal stress analysis, a material modification coefficient C was introduced. The final regression models for any fiber/resin system are summarized in Table 5.

Table 5: Regression models for typical composite structures

Angled structures

$$\Delta\phi = C_1(-0.826 + 0.951V_f)(180 - \phi)/90$$

Single-stiffener structures

$$\Delta\phi = C_2 \left[-0.073 - \left(0.003 + 0.040e^{-\frac{h}{1.264}} \right) r + 0.173(V_f - 0.49) \right]$$

Double-stiffener structures

$$\Delta\phi_v = C_2 \left[0.066 + 0.3e^{-\frac{h}{0.971}} + \left(0.016 + 0.121e^{-\frac{h}{1.207}} \right) r - 0.561(V_f - 0.49) \right]$$

Cylindrical shells

$$T_{cy} = 0.006C_1 \left[\phi/180 + (\phi/180)^2 \right] (1 - V_f) r$$

For angled structures and cylindrical shells, the coefficients can be estimated as

$$C_1 = \frac{(\alpha_T - \alpha_l)\Delta T / (1 + \alpha_T \Delta T)}{(\alpha_{T_0} - \alpha_{l_0})\Delta T_0 / (1 + \alpha_{T_0} \Delta T_0)} \quad (6)$$

where

α_i : in-plane CTE

α_T : through-thickness CTE

ΔT : temperature change

α_{i0} : reference in-plane CTE (E-glass/epoxy cross ply laminates)

α_{T0} : reference through-thickness CTE (E-glass/epoxy cross ply laminates)

ΔT_0 : reference temperature change (E-glass/epoxy cross ply laminates)

For stiffener structures, the coefficients can be estimated as

$$C_2 = \frac{\alpha_m \Delta T / (1 + \alpha_m \Delta T)}{\alpha_{m0} \Delta T_0 / (1 + \alpha_{m0} \Delta T_0)} \quad (7)$$

where

α_m : CTE of resin

α_{m0} : reference CTE (CTE of epoxy)

The material modification coefficients for some fiber/resin systems are shown in Table 6.

Table 6: Material modification coefficients for some fiber/resin systems (cross ply laminates)

| Fiber/resin system | Material modification coefficient | |
|--------------------|--|--|
| | Angled structures and cylindrical shells | Single-stiffener and double-stiffener structures |
| E-glass/epoxy | 1.00 | 1.00 |
| Carbon/epoxy | 1.38 | 1.00 |
| E-glass/polyester | 1.85 | 1.90 |
| Carbon/polyester | 2.36 | 1.90 |

4 ASSEMBLY ANALYSIS AND OPTIMIZATION

4.1 Structural Tree Method

After the deformation and tolerances of typical structures were studied and the regression models were obtained, they were used for assembly analysis and synthesis. The advantages are that it does not need the finite element analysis, thus the amount of computational efforts are greatly reduced. The structural tree method, a method based on structural analysis and coordinate transformation, was developed for assembly tolerance analysis and synthesis. The approach is as follows:

1. For a given composite assembly, from the origin, identify typical structures, e.g. L-shaped structures, single-stiffener structures...
2. Assign deformation feature points $\mathbf{N}_1 \dots \mathbf{N}_n$ based on typical structure study. Generally, these points are located at the curved part of these structures.
3. Construct the structural tree based on these points; each point will form a node of the tree



4. Using the regression models, determine the rotational angle ε_i of node i with reference to its prior node along the path; Formulate the conversion matrix $\mathbf{R}_{\mathbf{N}_i \mathbf{N}_{i-1}}$ as

$$\mathbf{R}_{N_i N_{i-1}} = \begin{bmatrix} \cos \varepsilon_i & -\sin \varepsilon_i \\ \sin \varepsilon_i & \cos \varepsilon_i \end{bmatrix}. \quad (8)$$

5. Formulate deformation relations for node \mathbf{N}_i as

$$\delta_{N_i} = \delta_{N_{i-1}} + \left[\prod_{j=1}^i \mathbf{R}_{N_j N_{j-1}} \right] (\mathbf{N}_i - \mathbf{N}_{i-1}) - (\mathbf{N}_i - \mathbf{N}_{i-1}) \quad (9)$$

i.e.

$$\delta_{N_i} = \left\{ \sum_{j=1}^i \left[\prod_{k=1}^j \mathbf{R}_{N_k N_{k-1}} \right] (\mathbf{N}_j - \mathbf{N}_{j-1}) \right\} - (\mathbf{N}_i - \mathbf{N}_0). \quad (10)$$

6. After the deformation and tolerances of all nodes are obtained, find the total deformation and tolerance of assembly.

A simple assembly composed of two L-shaped structures, as shown in Figure 14, was studied to validate this approach. Its structural tree is constructed in Figure 15.

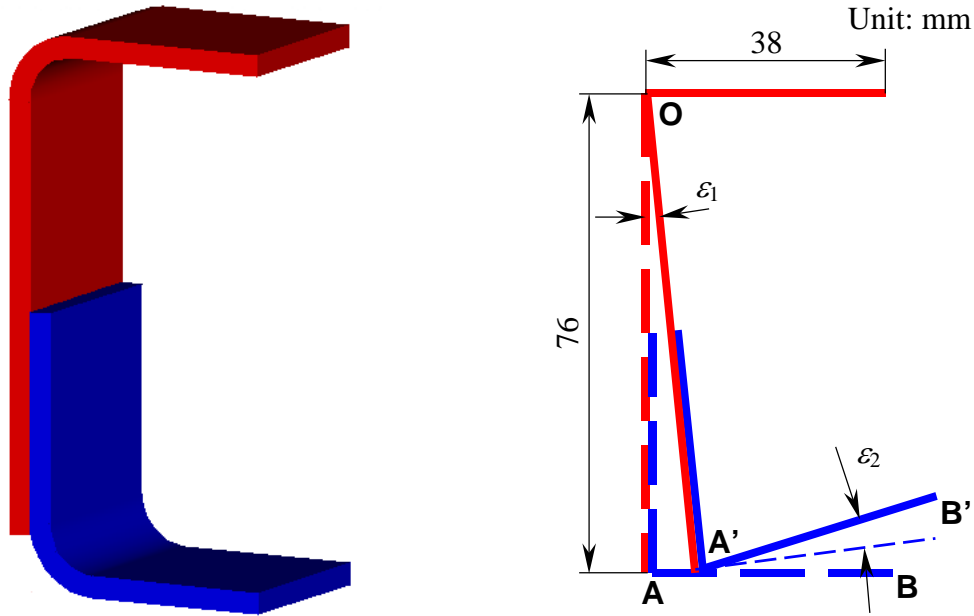


Figure 14: Assembly of two L-shaped structures



Figure 15: Structural tree of the assembly of two L-shaped structures

Using Equation 8, the rotational matrices were formulated as follows:

$$\mathbf{R}_{AO} = \begin{bmatrix} \cos \varepsilon_1 & -\sin \varepsilon_1 \\ \sin \varepsilon_1 & \cos \varepsilon_1 \end{bmatrix}$$

$$\mathbf{R}_{BA} = \begin{bmatrix} \cos \varepsilon_2 & -\sin \varepsilon_2 \\ \sin \varepsilon_2 & \cos \varepsilon_2 \end{bmatrix}.$$

The deformation of \mathbf{B} is derived according to Equation 10 as

$$\delta_{\mathbf{B}} = \mathbf{R}_{AO}(\mathbf{A} - \mathbf{O}) + \mathbf{R}_{BA} \mathbf{R}_{AO}(\mathbf{B} - \mathbf{A}) - \mathbf{B}.$$

When E-glass/epoxy cross ply laminates are considered and the fiber volume fraction is 49%, the displacement at \mathbf{B} is

$$\delta_{\mathbf{B}} = \begin{bmatrix} 76 \sin \varepsilon_1 - 38[1 - \cos(\varepsilon_1 + \varepsilon_2)] \\ 76(1 - \cos \varepsilon_1) + 38 \sin(\varepsilon_1 + \varepsilon_2) \end{bmatrix} = \begin{bmatrix} 0.48 \\ 0.48 \end{bmatrix}.$$

The total displacement at \mathbf{B} is $\|\delta_{\mathbf{B}}\|_2 = 0.68$ mm. In order to test the effectiveness of this method, the FEA analysis was also conducted. The displacement at \mathbf{B} from the FEA, as shown in Figure 16, is 0.72 mm, which shows the structural tree method can predict the assembly deformation of composites effectively.

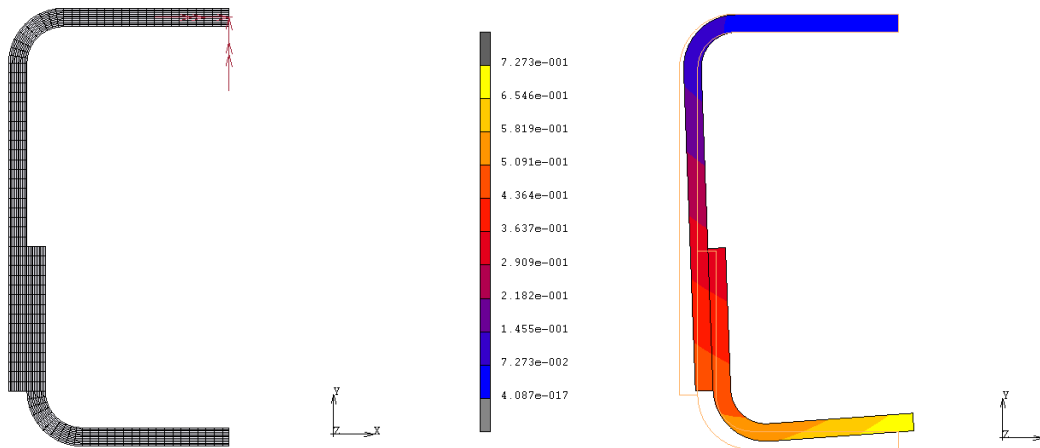


Figure 16: FEA analysis of assembly of two L-shaped structures

4.2 Case Study: Assembly of Two Single-Stiffener Structures and One Angled Structure

A complex assembly composed of two single-stiffener structures 1, 2 and an angled structure 3, as shown in Figure 17, was studied. Its corresponding structural tree is as shown in Figure 18.

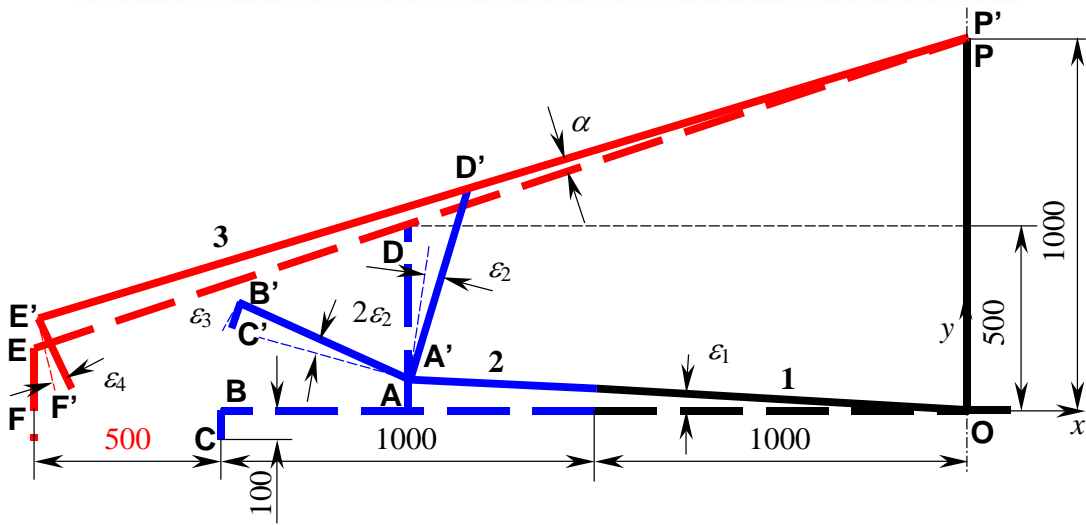
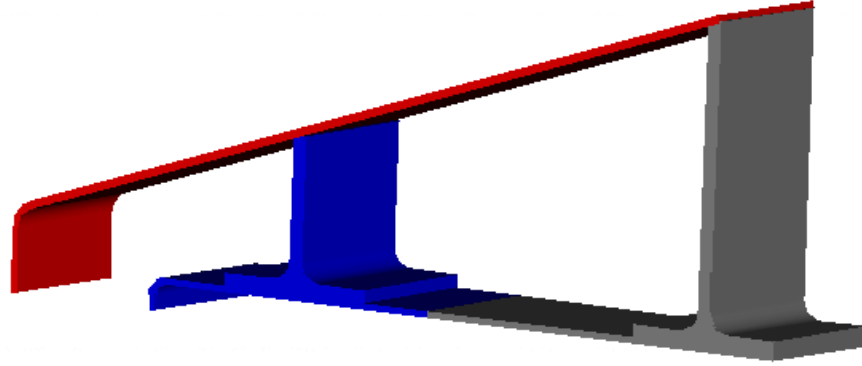


Figure 17: Assembly of two single-stiffener structures and one angled structure

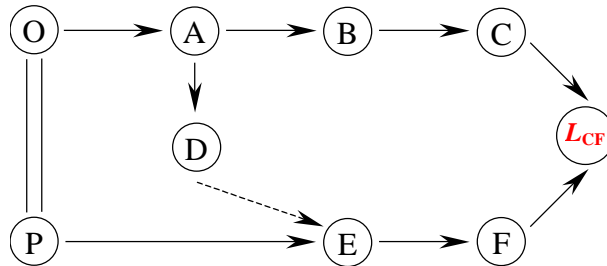


Figure 18: Structural tree for the assembly of two single-stiffener structures and one angled structure

In order to formulate the displacement at **F**, α needs to be calculated in the following procedure:

$$\mathbf{R}_{DA} = \begin{bmatrix} \cos \varepsilon_2 & \sin \varepsilon_2 \\ -\sin \varepsilon_2 & \cos \varepsilon_2 \end{bmatrix},$$

$$\mathbf{D}' = \mathbf{R}_{AO}(\mathbf{A} - \mathbf{O}) + \mathbf{R}_{DA}\mathbf{R}_{AO}(\mathbf{D} - \mathbf{A})$$

$$= \begin{bmatrix} -1500 \cos \varepsilon_1 + 500 \sin(\varepsilon_1 + \varepsilon_2) \\ 1500 \sin \varepsilon_1 + 500 \cos(\varepsilon_1 + \varepsilon_2) \end{bmatrix},$$

$$\alpha = \tan^{-1}[(y_P - y_D)/(x_P - x_D)] - \tan^{-1}[(y_P' - y_D')/(x_P' - x_D')].$$

The deformation relations for each branch are shown as follows, respectively. For simplification, all the spring-in angles take positive values. According to the STM, the rotational matrices and the displacement at **C** are:

$$\mathbf{R}_{AO} = \begin{bmatrix} \cos \varepsilon_1 & \sin \varepsilon_1 \\ -\sin \varepsilon_1 & \cos \varepsilon_1 \end{bmatrix},$$

$$\mathbf{R}_{BA} = \begin{bmatrix} \cos 2\varepsilon_2 & \sin 2\varepsilon_2 \\ -\sin 2\varepsilon_2 & \cos 2\varepsilon_2 \end{bmatrix},$$

$$\mathbf{R}_{CB} = \begin{bmatrix} \cos \varepsilon_3 & -\sin \varepsilon_3 \\ \sin \varepsilon_3 & \cos \varepsilon_3 \end{bmatrix},$$

$$\begin{aligned} \delta_C &= \mathbf{R}_{AO}(\mathbf{A} - \mathbf{O}) + \mathbf{R}_{BA}\mathbf{R}_{AO}(\mathbf{B} - \mathbf{A}) + \mathbf{R}_{CB}\mathbf{R}_{BA}\mathbf{R}_{AO}(\mathbf{C} - \mathbf{B}) - \mathbf{C} \\ &= \begin{bmatrix} -1500 \cos \varepsilon_1 - 500 \cos(\varepsilon_1 + 2\varepsilon_2) - 100 \sin(\varepsilon_1 + 2\varepsilon_2 - \varepsilon_3) + 2000 \\ 1500 \sin \varepsilon_1 + 500 \sin(\varepsilon_1 + 2\varepsilon_2) - 100 \cos(\varepsilon_1 + 2\varepsilon_2 - \varepsilon_3) + 100 \end{bmatrix}. \end{aligned}$$

The rotational matrices and the displacement at **F** are:

$$\mathbf{R}_{EP} = \begin{bmatrix} \cos \alpha & \sin \alpha \\ -\sin \alpha & \cos \alpha \end{bmatrix},$$

$$\mathbf{R}_{FE} = \begin{bmatrix} \cos \varepsilon_4 & -\sin \varepsilon_4 \\ \sin \varepsilon_4 & \cos \varepsilon_4 \end{bmatrix},$$

$$\begin{aligned} \delta_F &= \mathbf{R}_{EP}(\mathbf{E} - \mathbf{P}) + \mathbf{R}_{FE}\mathbf{R}_{EP}(\mathbf{F} - \mathbf{E}) - (\mathbf{F} - \mathbf{P}) \\ &= \begin{bmatrix} -2500 \cos \alpha - 833 \sin \alpha - 267 \sin(\alpha - \varepsilon_4) + 2500 \\ 2500 \sin \alpha - 833 \cos \alpha - 267 \cos(\alpha - \varepsilon_4) + 1100 \end{bmatrix}. \end{aligned}$$

The assembly deformation between point **F** and point **C** is

$$\delta_{L_{CF}} = \delta_C - \delta_F.$$

When $r = 6.35\text{mm}$, $h = 3.175\text{mm}$, the spring-in angles were computed using the non-linear regression models. The deformation was computed as $\delta_C = [0.05 \ 5.90]^T$ and $\delta_F = [-0.18 \ 3.44]^T$. Thus, $\delta_{L_{CF}} = [0.23 \ 2.46]^T$ and $\|\delta_{L_{CF}}\|_2 = 2.47$.

4.3 Design Optimization

When the design parameters are bounded, the assembly deformation can be minimized using the STM. Because of the non-linear nature of the regression-based dimensional variation model and the complex transformation relationship, non-linear programming is needed. Sequential quadratic programming was used in this study. Using the assembly of two single-stiffener structures and one angled structure as an example, the objective function and constraints are:

$$\text{Min } \|\delta_{L_{CF}}\|_2$$

s.t.

$$3 \leq r_1 \leq 12; \quad 3 \leq r_2 \leq 12; \quad 3 \leq r_3 \leq 12;$$

$$3 \leq h_1 \leq 3.25; \quad h_1 = h_2 = h_3;$$

$$0.45 \leq V_{f1} \leq 0.55; \quad 0.45 \leq V_{f2} \leq 0.55; \quad 0.45 \leq V_{f3} \leq 0.55.$$

After optimization, the assembly deformation is $\|\delta_{L_{cf}}\|_2 = 1.76$, as show in Table 7. It is shown that by modifying design geometric parameters, the assembly deformation can be reduced by 29%.

Table 7: Assembly design optimization

| | Original value | Optimized value |
|---------------------------|----------------|-----------------|
| r_1 (mm) | 6.35 | 6.37 |
| h_1 (mm) | 3.175 | 3.25 |
| V_{f1} | 0.49 | 0.55 |
| r_2 (mm) | 6.35 | 3.00 |
| h_2 (mm) | 3.175 | 3.25 |
| V_{f2} | 0.49 | 0.55 |
| r_3 (mm) | 6.35 | 6.35 |
| h_3 (mm) | 3.175 | 3.25 |
| V_{f3} | 0.49 | 0.45 |
| Assembly deformation (mm) | 2.47 | 1.76 |

5 CONCLUSIONS

In this paper, an innovative dimensional variation prediction method was developed. A dimensional variation model was first developed for process simulation based on thermal stress analysis and finite element analysis (FEA). This model was validated against the analytical solutions, the data from open literature, and the experiments. The results show that although there are certain errors in some cases, this model can predict the dimensional variations with adequate accuracy.

The regression-based dimensional variation model was developed based on the typical structure study using the developed FEA-based dimensional variation model. These typical structures include angled structures, single-stiffener structures, double-stiffener structures, cylindrical shells, hat shaped structures, structures with an open window, and 3-D stiffener structures were modeled. Data were collected by varying the design geometric parameters. Regression models were developed using the collected data. In order to make the non-linear regression models comprehensive, a material modification coefficient was introduced based on the analytical solution and FEA results. By incorporating this coefficient, the regression-based model can be applied to any fiber/resin type and/or any stacking sequence. The developed regression-based dimensional variation model does not require FEA, thus it significantly reduces the amount of computation time and provides a quick guide for composite product design.

The structural tree method was developed to compute the deformation of general shape composite components and composite assemblies the regression-based dimensional variation model. The advantage of this approach is that it does not need the finite element analysis, thus the amount of computation time is greatly reduced, which is crucial for practical applications. The methods presented in this paper provide a foundation to develop practical and proactive dimensional control techniques.

REFERENCES

- [1] Albert, C. and Fernlund, G., "Spring-in and Warpage of Angled Composite Laminates," *Composite Science and Technology*, 62(14): 1895-1912 (2002).
- [2] Radford, D.W. and Rennich, T.S., "Separating Sources of Manufacturing Distortion in Laminated Composites," *Journal of Reinforced Plastics and Composites*, 19(8): 621-641 (2000).
- [3] Svanberg, J. M. and Holmberg, J. A., "An Experimental Investigation on Mechanisms for Manufacturing Induced Shape Distortions in Homogeneous and Balanced Laminates," *Composites Part A*, 32(6): 827-838 (2001).
- [4] Jain, L.K. and Mai, Y.W., "On Residual Stress Induced Distortions during Fabrication of Composite Shells," *Proceedings of the 1995 10th Technical Conference of the American Society for Composites*, 261-270 (1995).
- [5] Jain, L.K. and Mai, Y.W., "On Residual Stress Induced Distortions during Fabrication of Composite Shells," *Journal of Reinforced Plastics and Composites*, 15(8): 793-805 (1996).
- [6] Jain, L.K. and Mai, Y.W., "Stresses and Deformations Induced during Manufacturing. Part I: Theoretical Analysis of Composite Cylinders and Shells," *Journal of Composite Materials*, 31(7) 673-695 (1997).
- [7] Jain, L.K., Lutton, B.G., Mai, Y.W. and Paton, R., "Stresses and Deformations Induced during Manufacturing. Part II: A Study of the Spring-in Phenomenon," *Journal of Composite Materials*, 31(7) 696-719 (1997).
- [8] Huang, C.K. and Yang, S.Y., "Warping in Advanced Composite Tools with Varying Angles and Radii," *Composites Part A*, 28A(9-10): 891-893 (1997).
- [9] Meink, T. and Shen, M.H.H., "Processing Induced Warpage in Composite Cylindrical Shells Part I," *12th Engineering Mechanics Conference* (1998).
- [10] Meink, T. and Shen, M.H.H., "Processing Induced Warpage in Composite Cylindrical Shells Part I," *ASME Winter Annual Meeting* (1998).
- [11] Meink, T. and Shen, M.H.H., "Processing Induced Warpage in Composite Cylindrical Shells," in *Advances in composite materials and mechanics*, ed. by Arup Maji, American Society of Civil Engineers, Reston, VA, 1-12 (1999).
- [12] Theriault, R. P., Osswald, T. A. and Castro, J.M., "Processing Induced Residual Stress in Asymmetric Laminate Panels," *Polymer Composites*, 20(3): 493-509 (1999).
- [13] Wiersma, H.W., Peeters, L.J.B. and Akkerman, R., "Prediction of Springforward in Continuous-Fiber/Polymer L-Shaped Parts," *Composites Part A*, 29A(11): 1333-1342 (1998).
- [14] Darrow, D.A., Jr. and Smith, L.V., "Evaluating the Spring-in Phenomenon of Polymer Matrix Composites," *33rd International SAMPE Technical Conference*, 33: 326-337 (2001).
- [15] Darrow, D.A., Jr. and Smith, L.V., "Isolating Components of Processing Induced Warpage in Laminated Composites," *Journal of Composite Materials*, 36(21): 2407-2419 (2002).
- [16] Golestanian, H. and El-Gizawy, A.S., "Modeling of Process Induced Residual Stresses in Resin Transfer Molded Composites with Woven Fiber Mats," *Journal of Composite Materials*, 35(1): 1513-1528 (2001).

- [17] Wang, J., Kelly, D. and Hillier, W., "Finite Element Analysis of Temperature Induced Stresses and Deformations of Polymer Composite Components," *Journal of Composite Materials*, 34(17): 1456-1471 (2000).
- [18] Fernlund, G., Nelson, K.M. and Poursartip, A., "Modeling of Process Induced Deformations of Composite Shell Structures," *45th International SAMPE Symposium and Exhibition*, 45(1): 169-177 (2000).
- [19] Ding, Y., Chiu, W.K. and Liu, X.L., "Anisotropy Related 'Spring-in' of Angled Composite Shells," *Polymers & Polymer Composites*, 9(6): 393-401 (2001).
- [20] Zhu, Q., Geubelle, P.H., Li, M. and Tucker, C.L., III, "Dimensional Accuracy of Thermoset Composites: Simulation of Process-Induced Residual Stresses," *Journal of Composite Materials*, 35(2): 2171-2205 (2001).
- [21] Dong, C.S., Zhang C., Liang, Z.Y., and Wang, B., "Dimensional Prediction and Control for Composite Assembly," *Proceedings of SAMPE 2003 (48th ISSE)*, Long Beach, CA (2003).
- [22] Dong, C.S., Zhang C., Liang, Z.Y., and Wang, B., "Dimensional Prediction and Control for Resin Transfer Molding Process," *Proceedings of the Fourth International Conference on Composite Science and Technology (ICCST/4)*, Durban, South Africa (2003).
- [23] Dong, C.S., Zhang C., Liang, Z.Y., and Wang, B., "Dimension Variation Prediction Control for Composites," submitted to *Composites, Part A*.